Timing Stability of TCSPC Experiments

W. Becker, A. Bergmann, Becker & Hickl GmbH, Berlin[1]

Abstract: Advanced time-correlated single-photon counting (TCSPC) devices are able to record several 10^6 photons per second and deliver an instrument response function down to 25 ps FWHM. Under these conditions the accuracy of fluorescence decay or photon migration times is limited by systematic timing errors rather than by the photon statistics. The experiments described below determined the variation of the instrument response function (IRF) with the count rate and the timing drift for an SPC-140 TCSPC module and a number of commonly used detectors. For count rates from $3 \cdot 10^4$ to $4 \cdot 10^6$ s^{-1} a shift of the first moment of the IRF smaller than 2 ps was obtained. The drift over 16 minutes was within ±0.7 ps.

Time-correlated single photon counting (TCSPC) is based on the detection of single photons of a periodic signal, the measurement of the detection times, and the build-up of the photon distribution over the time in the signal period [28]. Time-correlated single photon counting (TCSPC) is superior to analog recording techniques in terms of signal bandwidth, efficiency, and signal-to-noise ratio. However, early TCSPC setups had very limited count rates and correspondingly long acquisition times. The low count rate was a result of the low repetition rates of the light sources and the slow processing speed of the electronics of that time. Moreover, the classic TCSPC technique was intrinsically one-dimensional, i.e. restricted to the recording of the waveform of a single signal.

Advanced TCSPC techniques are multi-dimensional, i.e. are able to record the photon distribution not only versus the time in the signal period, but also versus wavelength [4, 8, 9], spatial coordinates [3, 6], the time from the start of the experiment [2], or other variables [22, 29, 30]. Multi-dimensional recording requires a substantially higher number of photons than simple waveform recording. In the last ten years the count rates of TCSPC devices have been increased by more than two orders of magnitude [2, 3, 7]. Currently used TCSPC setups can be operated at count rates of several 10^6 photons per second. Simultaneously, light sources with high repetition rate and pulse widths in the picosecond and femtosecond range became commonly available and affordable. The instrument response function (IRF), i.e. the response of the detection system to the excitation pulse, can be as short as 25 ps. The short IRF in conjunction with a high and often variable count rate poses significant requirements to the timing stability of the detectors and the TCSPC electronics.

Theoretical time-resolution of TCSPC measurements

Typical examples of TCSPC experiments are fluorescence lifetime measurements and measurements of the scattering and absorption coefficients in turbid media. In both cases the sample is excited by short light pulses, and the waveform of the light emitted by the sample is measured. The statistical accuracy of the measurement can be estimated by using the first moment, M_1 of the photon distribution. The first moment, M_1, or the 'centroid' of the function $f(t)$ is defined as

$$M_1 = \frac{\int t \; f(t) dt}{\int f(t) dt}$$

For discrete time channels containing discrete numbers of photons M_1 is

[1] Correspondence: becker@becker-hickl.com, bergmann@becker-hickl.com

$$M_1 = \frac{\sum N_i \, t_i}{N}$$

with ti = time of time channel i
Ni = number of photon in time channel i
N = total number of photons

M_1 can also be interpreted as the average arrival time of all photons within a TCSPC measurement. It is thus linearly related to the time-constant of a single-exponential sample response, e.g. the lifetime of a single-exponential fluorescence decay. The standard deviation of the first moment, σ_{M1}, and thus he standard deviation, σ_τ of the sample time constant, τ, are

$$\sigma_{M1} = \sigma_\tau = \tau / \sqrt{N}$$

This is the known expression of the accuracy of a fluorescence lifetime measured with an infinitely short IRF, a large number of time channels, and a time-channel width much shorter than the fluorescence lifetime, τ, and negligible background. As a typical example, from 10^6 photons a lifetime of 1 ns can ideally be derived with an standard deviation of 1 ps.

In practice the measured waveform is the convolution of the sample response and the IRF. If two functions are convoluted the first moments of both functions add linearly. From the recordings of a fluorescence decay and the corresponding IRF the fluorescence lifetime, τ, can be derived by

$$\tau = M_{1\,fluor} - M_{1IRF}$$

with M_{1flour} = first moment of the fluorescence recording
and $M1_{IRF}$ = first moment of the IRF recording

The relation can be used to estimate the shortest fluorescence lifetime that can be obtained from a given number of photons in a system of a given IRF. Let the standard deviation of the photon arrival times in the IRF recording be σ_{IRF}. The standard deviation of the first moment, σ_{M1}, of the IRF is then

$$\sigma_{M1} = \sigma_{IRF} / \sqrt{N}$$

For fluorescence lifetimes much shorter than the IRF width the shapes of the recorded IRF and the recorded fluorescence curve are almost identical. Provided the same number of photons, N, is recorded both in the IRF and the fluorescence curve the standard deviation, σ_τ, of the calculated τ is:

$$\sigma_\tau = \sqrt{2}\, \sigma_{IRF} / \sqrt{N}$$

With a femtosecond laser and an MCP PMT σ_{irf} is about 10 ps. For a total number of recorded photons of $N = 10^6$ both in the IRF and the fluorescence - which is certainly a conservative assumption - the standard deviation of a short lifetime is 14 fs. A statistical accuracy on the level of a several 10 fs is indeed confirmed by distance measurements based on TCSPC [26, 27].

Under typical conditions the systematic timing errors in a TCSPC system are much larger than 14 fs. Errors may be introduced by variations of the temperature and operating voltage in the detector and the electronic system, and, more important, by changes in the count rate. The most critical parts of the system are the PMT and its voltage divider. Changes in the count rate induce changes in the voltage distribution across the dynodes and, consequently, changes in the transit time.

Test of the timing stability of a real TCSPC system

The timing stability of a typical TCSPC device in combination with commonly used detectors was tested in the setup shown in Fig. 1.

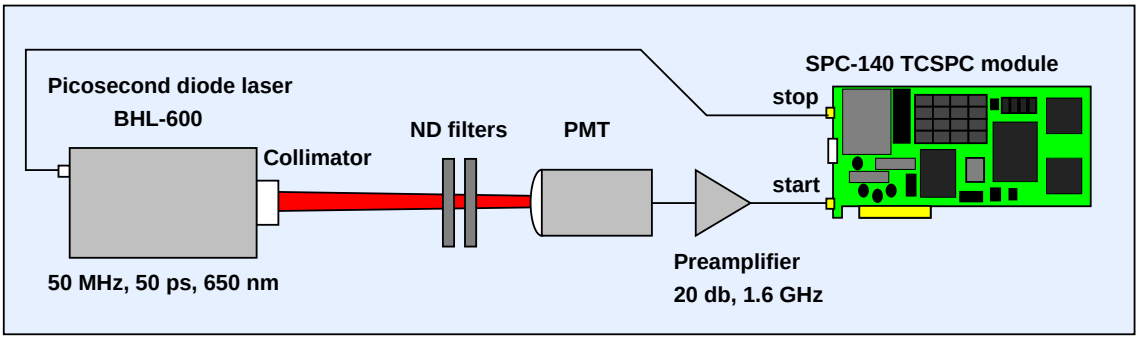

Fig. 1: Test setup

A BHL-600 picosecond diode laser (Becker & Hickl) was used as a test light source. It delivers pulses of about 50 ps FWHM at a wavelength of 650 nm and a repetition rate of 50 MHz. The light was attenuated by a package of ND filters and sent onto the active area of the PMT. The intensity was changed by replacing the filters in the beam path. To keep the effective optical path length constant filters were replaced with filters of equal thickness only. The single-photon pulses of the PMT were amplified and used as start pulses of a Becker & Hickl SPC-140 TCSPC module. The stop pulses came from the reference output of the diode laser. Due to its short dead time of 100 ns the SPC-140 the setup can be used to test the timing performance of different detectors for effective count rates up to about $5 \cdot 10^6$ s^{-1}.

Dependence of the IRF on the count rate

Fig. 2 shows the count-rate dependent shift of the IRF for an Amperex XP2020 linear-focused PMT. The XP2020 is used in large numbers in nuclear instrumentation and is still something like a reference standard for high-current short-time PMTs. The XP2020 is characterised by a high operating voltage of 2.2 to 2.7 kV, an extremely high gain, and a total transit time of about 28 ns. It delivers a single-electron response (SER) of 50 to 100 mV average amplitude and 3 to 5 ns width. Due to the high amplitude of the pulses, the XP2020 was connected directly, i.e. without a preamplifier, to the TCSPC module.

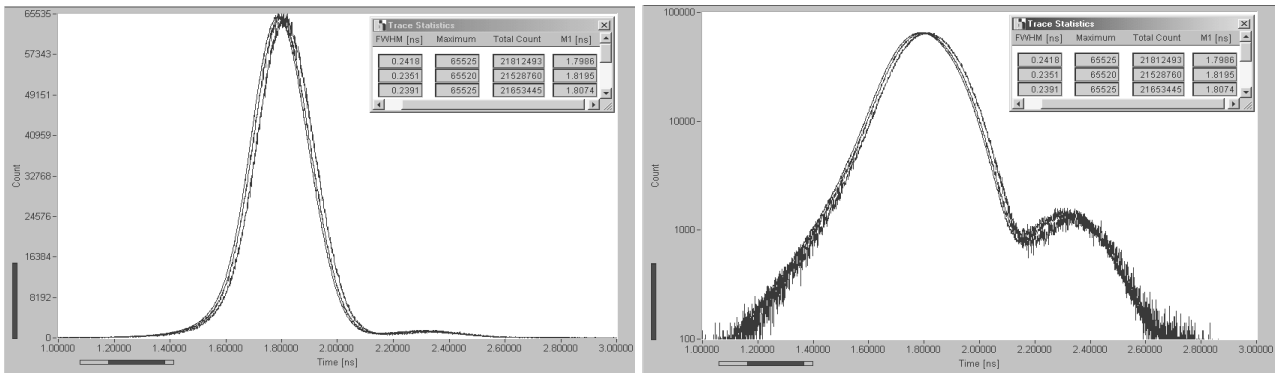

Fig. 2: IRF of an XP2020 PMT for count rates of 1 MHz, 100 kHz, and 500 kHz in linear scale (left) and logarithmic scale (right). The shift in M_1 between 100 kHz and 1 MHz count rate is 20 ps.

The first moment of the IRF shifts by about 20 ps when the count rate changes from 100 kHz to 1 MHz. The source of this shift is most likely the long transit time in conjunction with the high gain and the relatively large SER width. The high gain and the large SER width result in a relatively high output current at a given count rate. The result is a distortion in the voltage distribution at the dynodes which, in conjunction with the long transit time, results in a correspondingly large change in the IRF.

Better results can be expected for miniature PMTs, such as the Hamamatsu R5600 and R7400. These PMTs have a transit time of about 5.4 ns, an SER width of about 1.5 ns, and an average SER amplitude of a few 10 mV [14]. The short SER results in a correspondingly small anode current at a given count rate, and the low transit time in a correspondingly low transit-time change with the dynode voltages. R5600 or R7400 tubes are contained in the Hamamatsu H5773, H5783, and H7422 photosensor modules [16, 17]. A test result for a Hamamatsu H5773P-20 photosensor module is shown in Fig. 3.

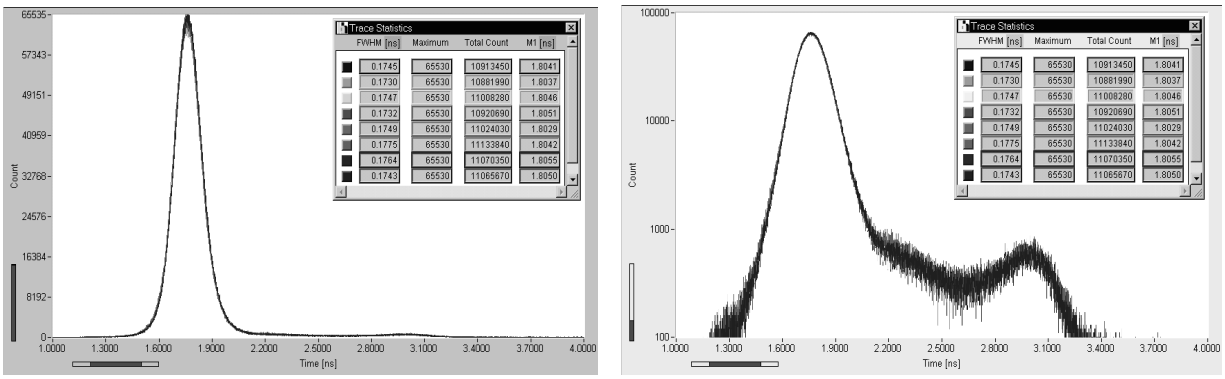

Fig. 3: IRF of an H5773-20 photosensor module for count rates of 30 kHz, 300 kHz, and 4 MHz in linear scale (left) and logarithmic scale (right). The shift between 30 kHz and 4 MHz recorded count rate is <2 ps and not discernible in the IRF curves.

Indeed the module has an almost undetectable timing shift. For (recorded) count rates varying from 30 kHz to 4 MHz the shift in the first moment of the IRF is <2 ps and not discernible in the IRF curves. The surprisingly high timing stability may in part be a result of the Cockroft-Walton voltage-divider design of the H5773 modules [16].

The fastest detectors currently available for TCSPC are multichannel plate (MCP) PMTs [23]. MCP PMTs are commonly believed to be unable to work at count rates higher than a few 10^4 photons per second. Fig. 4, left, shows the IRF of a Hamamatsu R3809U MCP [15] for count rates of 100 kHz, 1.4 MHz, and 3.3 MHz for an illuminated area of 10 mm^2. There is indeed a considerable change in the IRF, with a shift in the first moment of almost 20 ps. The IRF shift is most likely an effect of the saturation of the microchannels. At high detector gain the output of a single microchannel saturates when a single photon enters the input [23]. The recovery time of the channel is in the microsecond range. If a large number of photoelectrons is concentrated on a limited number of microchannels these do not fully recover, and the IRF changes.

A simple extrapolation from the spot area of 10 mm^2 in Fig. 4, left, to smaller areas shows that the useful count rate can indeed be in the 10-kHz range. On the other hand, a substantially improved IRF stability can be expected for illumination of the full cathode area of 120 mm^2. IRF curves measured with illumination of the full cathode area are shown in Fig. 4, right. The response remains stable up to more than 3 MHz recorded count rate, with a shift in the first moment of less than 3 ps.

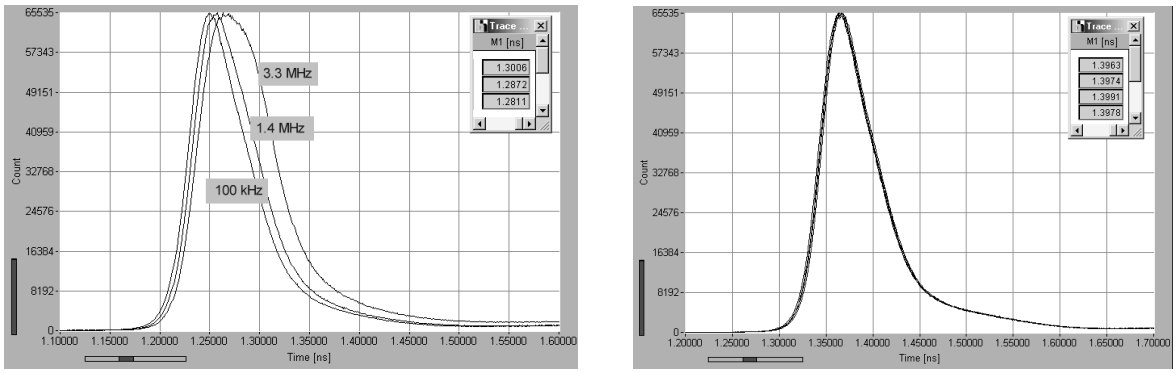

Fig. 4: IRF of an R3809U MCP-PMT for different count rates. Illumination by diode laser, pulse width 50 ps. Operating voltage -3 kV, 20 dB preamplifier gain, CFD threshold 80 mV. Left: Illuminated spot of 2 x 5 mm, recorded count rates 100 kHz, 1.4 MHz, 3.3 MHz. Right: Full cathode area illuminated, recorded count rates 3.3 MHz, 1.8 MHz, 480 kHz, and 25 kHz

These results show that MCP PMTs can be used for count rates up to the maximum useful count rate of currently available TCSPC systems. It should be noted, however, that the output current at a count rate of 3.3 MHz and an operating voltage of 3 kV is considerably higher than the maximum rating of 100 nA specified by the manufacturer. This is certainly not a problem in applications where high count rates appear only temporarily, like in scanning microscopy. The lifetime of the MCP at a continuous count rate of more than 3 MHz is not known.

The count-rate-dependent shift of the first moment found for frequently used detectors is summarised in the table below.

PMT Type	**Operating Voltage (Gain Control Voltage)**	**Voltage Divider Current**	**Count Rate MHz (recorded)**	**IRF width**	**Shift of M1 peak-peak**
XP2020	-2.5 kV	4 mA	0.1 to 1	230 ps	20
R5600	-0.9 kV	1 mA	0.03 to 4	175 ps	5 ps
H7422	(0.78 V)	N.A.	0.03 to 4	300 ps	8 ps
H5773/83	(0.9 V)	N.A.	0.03 to 4	175 ps	<2 ps
R3809U	-3 kV	75 µA	0.03 to 3.3	30 ps	<3 ps

IRF drift over time

The IRF stability of the TCSPC system over time is shown in Fig. 5 and Fig. 6. After 30 minutes of warm up, a series of 16 IRF curves was recorded over 16 minutes. Fig. 5 shows the results for an H5773-20 module. The count rate was 250 kHz.

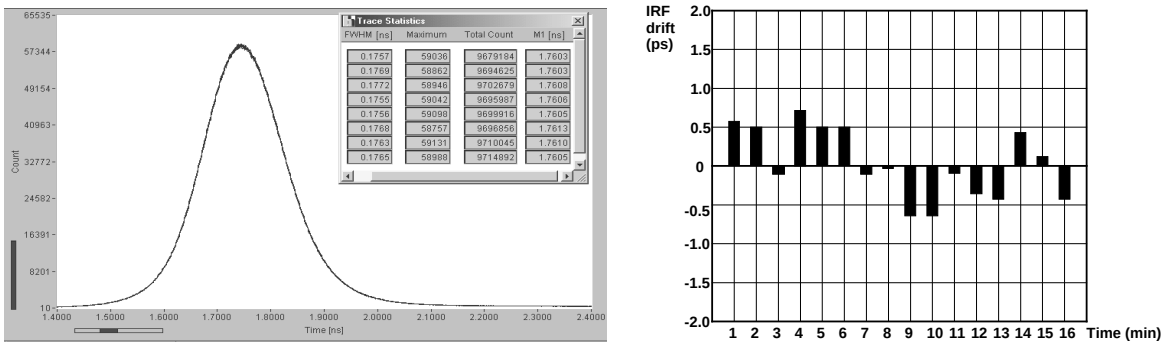

Fig. 5: Series of IRF recordings for an H5773-20 (left) and drift of the first moment (right). 16 consecutive recordings of 45 s over 16 minutes

The drift is so small that it is not discernible in the IRF curves. The drift of the first moment of the IRF recordings is within ± 0.7 ps. Surprisingly, the timing stability obtained with an R3809U MCP PMT is about a factor of two worse. The results are shown in Fig. 6.

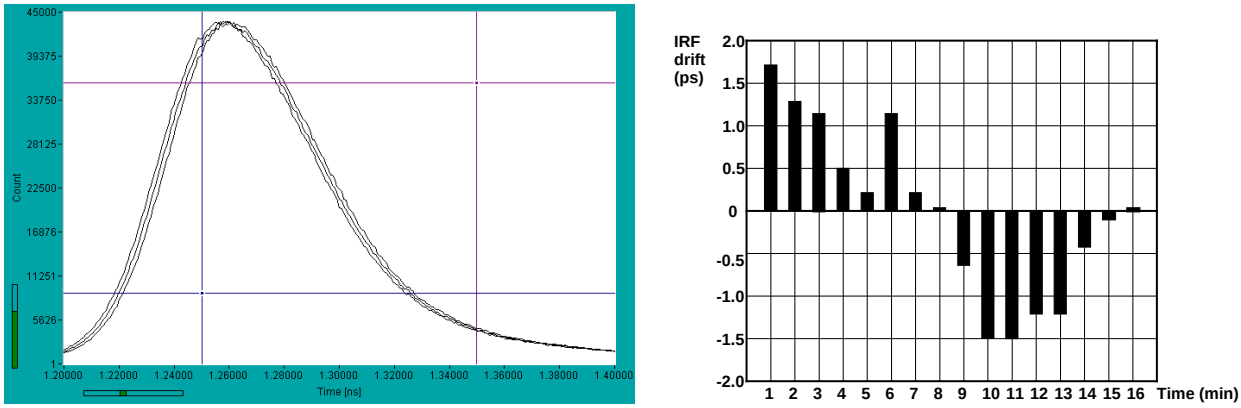

Fig. 6: Series of IRF recordings for an R3809U (left) and drift of the first moment (right). 16 consecutive recordings of 45 s over 16 minutes. Please note the different time scale compared to Fig. 5.

The drift in the first moment is about ± 1.5 ps, i.e. about twice as large as for the H5773. The reason is certainly not the MCP itself. Instability of the high voltage is also unlikely to cause the drift. At the operating voltage of 3 kV a change of 30 V in the voltage would be required for a shift of 3 ps. The most likely reason that the R3809 does not reach the stability of the H5773 is the lower gain. Slight changes in the CFD offset in the TCSPC module have therefore a larger influence on the timing.

Conclusions

TCSPC systems are able to maintain a timing stability of the order of 1 ps over a range of count rates from a few kHz to several MHz. The remarkably small dependence of the IRF on the intensity is particularly interesting for biomedical applications. These applications are often characterised by large intensity fluctuations which may be induced by physiological effects, by diffusion effects, or simply by a scanning procedure used to obtain images from a sample. In autofluorescence lifetime spectroscopy of tissue and time-resolved laser scanning microscopy a lifetime stability on the 10 ps scale is required to obtain FRET distances or local environment parameters independently of the variable fluorophore concentration [1, 5, 6, 10, 13, 20, 21]. An even higher timing stability is required in diffuse optical tomography [11, 12, 18, 19]. Haemodynamic effects cause changes in the first moment on the 1-ps level. The changes occur on a time scale of about one second, possibly even faster. Thus, a high number of photons must be acquired within measurement time intervals of the order of 100 ms. It has indeed been shown that TCSPC is able to track haemodynamic changes down to this level, independently from changes in the intensity [24, 25]. Other applications are intensity-induced lifetime changes of the chlorophyll in living plants or plant cells, electro-physiologial experiments on the cell level, and fluorescence correlation spectroscopy (FCS), fluorescence intensity distribution analysis (FIDA), and burst-integrated fluorescence lifetime experiments on the single-molecule level.

References

1. Bacskai, B.J., Skoch, J., Hickey, G.A., Allen, R., Hyman, B.T., Fluorescence resonance energy transfer determinations using multiphoton fluorescence lifetime imaging microscopy to characterize amyloid-beta plaques. J. Biomed. Opt 8, 368-375 (2003)
2. Becker, W., Hickl, H., Zander, C., Drexhage, K.H., Sauer, M., Siebert, S., Wolfrum, J., Time-resolved detection and identification of single analyte molecules in microcapillaries by time-correlated single photon counting. Rev. Sci. Instrum. 70, 1835-1841 (1999)
3. Becker, W., Bergmann, A., Wabnitz, H., Grosenick, D., Liebert, A., High count rate multichannel TCSPC for optical tomography. Proc. SPIE 4431, 249-245 (2001)
4. Becker, W., Bergmann, A., Biskup, C., Zimmer, T., Klöcker, N., Benndorf, K., Multi-wavelength TCSPC lifetime imaging. Proc. SPIE 4620, 79-84 (2002)
5. Becker, W., Bergmann, A., Biskup, C., Kelbauska, L, Zimmer, T., Klöcker, N., Benndorf, K., High resolution TCSPC lifetime imaging. Proc. SPIE 4963, 175-184 (2003)
6. Becker, W., Bergmann, A., Hink, M.A., König, K., Benndorf, K., Biskup, C., Fluorescence lifetime imaging by time-correlated single photon counting. Micr. Res. Techn. 63, 58-66 (2004)
7. W. Becker, A. Bergmann, G. Biscotti, K. Koenig, I. Riemann, L. Kelbauskas, C. Biskup High-Speed FLIM Data Acquisition by Time-Correlated Single Photon Counting. Proc. SPIE 5323, 27-36 (2004)
8. W. Becker, A. Bergmann, G. Biscotti, A. Rück, Advanced time-correlated single photon counting technique for spectroscopy and imaging in biomedical systems. Proc. SPIE 5340, 104-112 (2004)
9. Bird, D.K., Eliceiri, K.W., Fan, C-H., White, J.G., Simultaneous two-photon spectral and lifetime fluorescence microscopy. Appl. Opt. 43, 5173-5182 (2004)
10. Biskup, C., Kelbauskas, L., Zimmer, T., Benndorf, K., Bergmann, A., Becker, W., Ruppersberg, J.P., Stockklausner, C., Klöcker, N., Interaction of PSD-95 with potassium channels visualized by fluorescence lifetime-based resonance energy transfer imaging. J. Biomed. Opt. 9, 735-759 (2004)
11. Cubeddu, R., Pifferi, A., Taroni, P., Torricelli, A., Valentini, G., Compact tissue oximeter based on dual-wavelength multichannel time-resolved reflectance. Appl. Opt. 38, 3670-3680 (1999)
12. Cubeddu, R., Pifferi, A., Taroni, P., Torricelli, A., Valentini, G., Noninvasive absorption and scattering spectroscopy of bulk diffuse media: An application to the optical characterization of human breast. Appl. Phys. Lett. 74, 874-876 (1999)
13. Duncan, R. R., Bergmann, A., Cousin, M. A., Apps, D. K., Shipston, M. J., Multi-dimensional time-correlated single-photon counting (TCSPC) fluorescecne lifetime imaging microscopy (FLIM) to deetct FRET in cells. J. Microsc. 215(1), 1-12 (2004)
14. Hamamatsu Photonics K.K. (2001), R7400 Series Metal package photomultiplier tube
15. Hamamatsu Photonics K.K. (2001), R3809U-50 series Microchannel plate photomultiplier tube (MCP-PMTs)
16. Hamamatsu Photonics K.K. (2001), H5773/H5783/H6779/H6780/H5784 Photosensor modules
17. Hamamatsu Photonics K.K. (2003), H7422 series Metal package PMT with cooler - photosensor modules
18. Hebden, J.C., Schmidt, E.W., Fry, M.E., Schweiger, M., Hillman, E.M.C., Delpy, D.T., Simultaneous reconstruction of absorption and scattering images by multichannel measurement of purely temporal data. Opt. Lett. 24, 534-536 (1999)
19. Hebden, J.C., Gibson, A., Austin, T., Yusof, R.M., Everdell, N., Delpy, D.T., Arridge, S.R., Meek, J.H., Wyatt, J.S., Imaging changes in blood volume and oxygenation in the newborn infant brain using three-dimensional optical tomography. Phys. Med. Biol. 49, 1117-1130 (2004)
20. König K., Riemann I., High-resolution multiphoton tomography of human skin with subcellular spatial resolution and picosecond time resolution. J. Biom. Opt. 8, 432-439 (2003)
21. König, K., Riemann, I., Ehrlich, G., Ulrich, V., Fischer, P., Multiphoton FLIM and spectral imaging of cells and tissue. Proc. SPIE 5323, 240-251 (2004)
22. Kozlov, K.V., Wagner H.-E., Brandenburg R., Michel P., Spatio-temporally resolved spectroscopic diagnostics of the barrier discharge in air at atmospheric pressure. J. Phys. D: Appl. Phys. 34, 3164-3176 (2001)
23. Kume, Hidehiro (Chief Editor), Photomultiplier Tube. Hamamatsu Photonics K.K., 1994
24. Liebert, A., Wabnitz, H., Grosenick, D., Möller, M. Macdonald, R., Rinneberg, H., Evaluation of optical properties of highly scattering media by moments of distributions of times of flight of photons. App. Opt. 42, 5785-5792 (2003)
25. Liebert, A., Wabnitz, H., Steinbrink, J., Obrig, H., Möller, M., Macdonald, R., Villringer, A., Rinneberg, H., Time-resolved multidistance near-infrared spectroscopy at the human head: Intra- and extracerebral absorption changes from moments of distribution of times of flight of photons. Appl. Opt. 43, 3037-3047 (2004)
26. Massa, J.S., Buller, G.S., Walker, A.C., Smith, G., Cova, S., Umasuthan, M., Wallace, A.M., Optical design and evaluation of a three-dimensional imaging and ranging system based on time-correlated single-photon counting. Appl. Opt., 41:1070-1063 (2002)

27. Massa, J.S., Buller, G.S., Walker, A.C., Cova, S., Umasuthan, M., Wallace, A.M., Time-of-flight optical ranging system based on time-correlated single photon counting. Appl. Opt. 37(31) 7298-7304 (1998)
28. O'Connor, D.V., Phillips, D., Time Correlated Single Photon Counting, Academic Press, London, 1984
29. Wagner H.E., Brandenburg R., Kozlov K.V., Sonnenfeld A., Michel P., Behnke J.F., The barrier discharge: Basic properties ans applications to surface treatment. Vacuum 71, 417-436 (2003)
30. Wagner H.E., Brandenburg R., Kozlov K.V., Progress in the visualisation of filametary gas discharges, part1: Milestones and diagnostics of dielectric-barrier discharges by cross-correlation. Journal of Advanced Oxidation Technologies 7, 11-19 (2004)